

Formation of Colloidal Silver Nanoparticles: Capping Action of Citrate

Arnim Henglein*

Radiation Laboratory, University of Notre Dame, Notre Dame, Indiana 46556

Michael Giersig

Hahn-Meitner Institut, 14109 Berlin, Germany

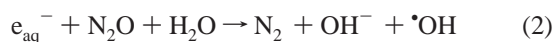
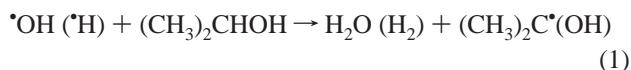
Received: July 22, 1999; In Final Form: September 5, 1999

Colloidal silver sols of long-time stability are formed in the γ -irradiation of 1.0×10^{-4} M AgClO_4 solutions, which also contain 0.3 M 2-propanol, 2.5×10^{-2} M N_2O , and sodium citrate in various concentrations. The reduction of Ag^+ in these solutions is brought about by the 1-hydroxyalkyl radical generated in the radiolysis of 2-propanol; citrate does not act as a reductant but solely as a stabilizer of the colloidal particles formed. Its concentration is varied in the range from 5.0×10^{-5} to 1.5×10^{-3} M, and the size and size distribution of the silver particles are studied by electron microscopy. At low citrate concentration, partly agglomerated large particles are formed that have many imperfections. In an intermediate range (a few 10^{-4} M), well-separated particles with a rather narrow size distribution and little imperfections are formed, the size slightly decreasing with increasing citrate concentration. At high citrate concentrations, large lumps of coalesced silver particles are present, due to destabilization by the high ionic strength of the solution. These findings are explained by two growth mechanisms: condensation of small silver clusters (type-I growth), and reduction of Ag^+ on silver particles via radical-to-particle electron transfer (type-II growth). The particles formed in the intermediate range of citrate concentration were studied by high-resolution electron microscopy and computer simulations. They constitute icosahedra and cuboctahedra.

Introduction

In the classical "Turkevich" preparation of colloids of precious metals, such as gold,¹ palladium,² and silver,³ sodium citrate is used as both the reducing agent and stabilizer of the particles formed. One can hardly distinguish between these two actions of citrate, since a variation in its concentration may cause both a change in the reduction rate and in the nucleation-to-growth ratio. Moreover, the oxidation/decarboxylation products of citrate, such as acetone dicarboxylic and itaconic acids, may be chemisorbed and affect the particle growth. In the present paper, the capping of silver particles by citrate is investigated under conditions where citrate does not contribute to the reduction of the Ag^+ ions. This situation is realized in the γ -radiolytic reduction of Ag^+ ions in aqueous solution in the presence of an alcohol.

The solution contains 1.0×10^{-4} M AgClO_4 , 2.5×10^{-2} M N_2O , 0.3 M 2-propanol, and citrate in various concentrations (5.0×10^{-5} to 1.5×10^{-3} M). The hydrated electrons, $\bullet\text{OH}$ radicals, and $\bullet\text{H}$ atoms, which are generated in the radiolysis of the aqueous solvent, are rapidly scavenged by the two solutes that are present in relatively high concentrations:



The organic radicals formed in these reactions reduce the silver ions. These radicals are generated at the same rate regardless of variations in the concentration of the dissolved substances

(which is an important advantage of using radiation in kinetic studies). Citrate does not react with e_{aq}^- ; it is also not attacked by $\bullet\text{OH}$ and $\bullet\text{H}$, since these radicals are efficiently scavenged (eq 1) at the rather high 2-propanol concentration used. Thus, citrate is solely a spectator to the ongoing redox processes. However, it plays an important role as stabilizer; clear yellow sols are obtained only in its presence, whereas gray solutions or precipitated silver results in its absence. In the present paper, information about its capping action is obtained by studying the size and size distribution of the silver particles formed at various citrate concentrations, as well as their absorption spectra. Moreover, the structure and shape of some particles are investigated by high-resolution electron microscopy and computer simulations.

Experimental Section

A 50 mL solution was irradiated in a closed 100 mL glass vessel. Prior to irradiation, the solution was bubbled with nitrous oxide. The vessel carried a sidearm with a 1 cm optical cuvette; spectra could therefore be measured without bringing the solution into contact with air. Irradiations were carried out in a commercial ^{60}Co γ source at a dose rate of 9.3×10^4 rad/h. During irradiation, the solutions became yellow and the plasmon absorption band of silver developed in the 380–430 nm range. The irradiation time was 65 min. At this point, all the Ag^+ ions had been reduced; this was concluded from the fact that the absorption band did not increase upon further irradiation.

The samples were observed in high-resolution transmission electron microscopes, Phillips 12 and JEOL 4000, operating at 120 respectively 200 kV. The quality of the lattice images was improved using the conditions of minimum phase contrast according to Kunath.⁴ Samples were prepared by putting a copper–carbon grid on a drop of the solution on oil paper and

* To whom correspondence should be addressed.

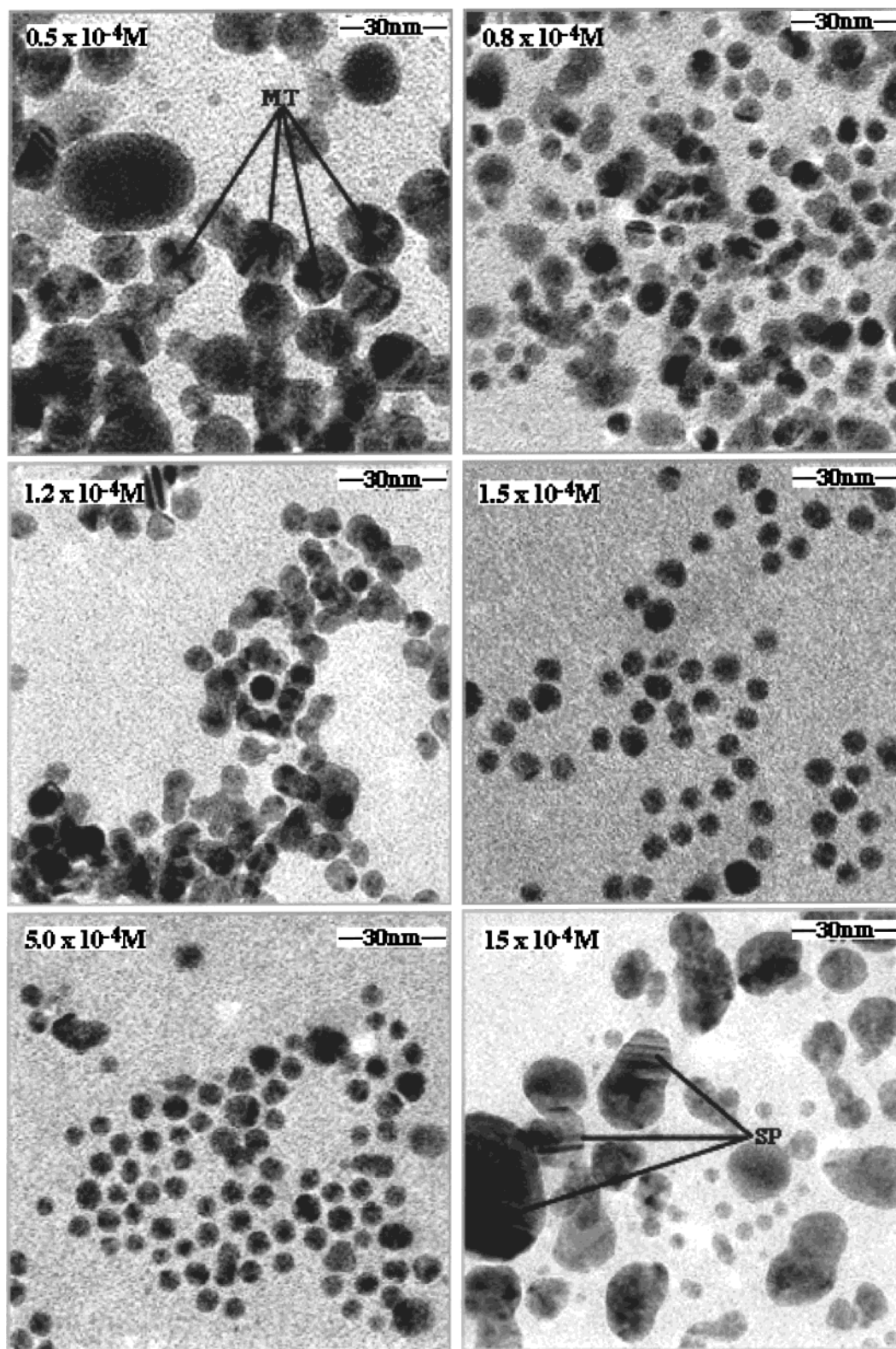


Figure 1. Electron micrographs at various citrate concentrations. MT: multiple twinned particles. SP: particles with staple faults.

letting the drop dry almost completely. The grid was then dried and stored in a desiccator.

Particle sizes are given as diameter or atom number per particle.

Results

Figure 1 shows electron micrographs for different citrate concentrations. Size distributions of a few samples are shown in Figure 2; these diagrams contain the entity $s = 100(\sum \Delta_i n_i) /$

$(d_m \sum n_i)$ as a measure of the size distribution ($\Delta_i = |d_i - d_m|$; d_i = particle diameter). The mean atom number of the particles, n , is calculated from the relation

$$n = \frac{0.5\pi N_A d_m^3}{3V_m} \quad (3)$$

assuming spherical particle shape (d_m is the mean particle diameter, V_m is the molar volume of silver; with $V_m = 10.5$

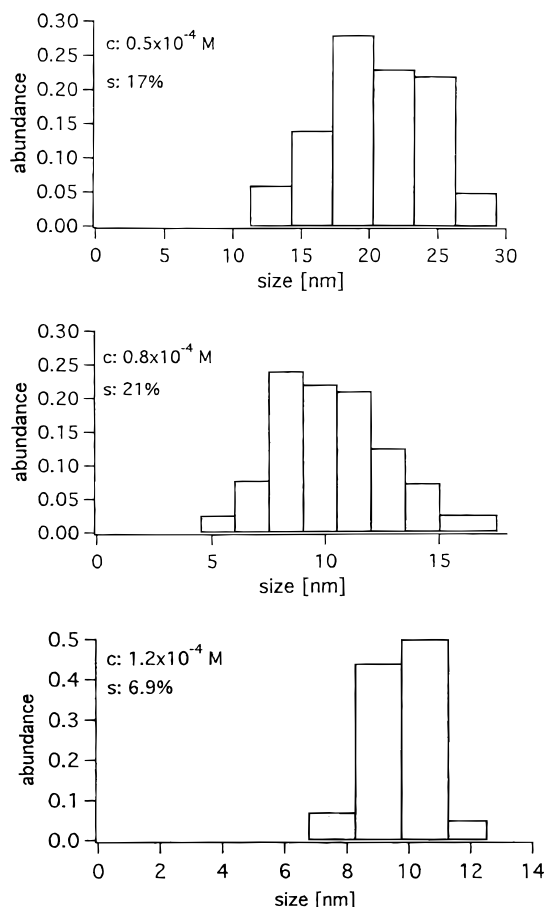


Figure 2. Size distributions of samples shown in Figure 1 in the transition from regimes 1 to 2. A total of 150 particles were counted in each case. Large lumps were not considered. *c*: citrate concentration. *s*: relative width of the size distribution.

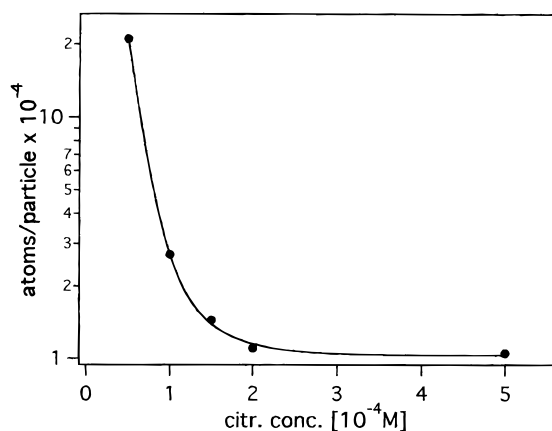


Figure 3. Particle size as expressed by the mean atom number per particle as a function of citrate concentration.

mL mol^{-1} and d_m in nm, $n = 30.4d_m^3$). In Figure 3, this number is plotted versus the citrate concentration. Typical absorption spectra are shown in Figure 4.

Citrate is an efficient stabilizer; all the solutions were clear and long-lived for weeks in the absence of air. However, depending on its concentration, citrate has a strong influence on the size and structure of the silver particles formed. Various concentration regimes can be distinguished in Figures 1–3.

(1) At the lowest citrate concentration of $0.5 \times 10^{-4} \text{ M}$, the size (atom number) is large and many particles stick together. The size distribution, *s*, is wide and even increases a little as

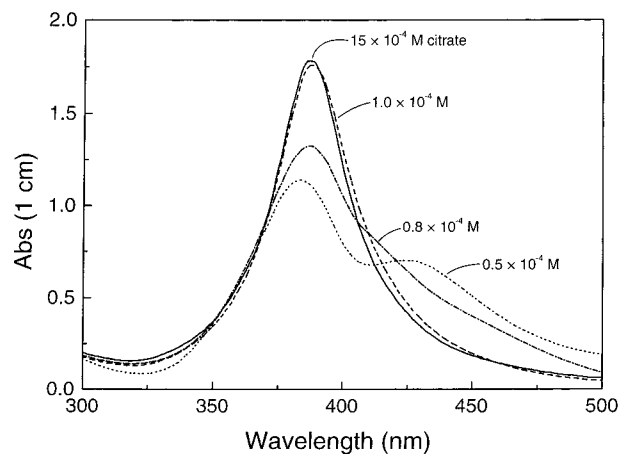


Figure 4. Absorption spectra of colloids obtained at various citrate concentrations.

one moves to $0.8 \times 10^{-4} \text{ M}$ citrate, where the particles are substantially smaller but still stick together frequently.

(2) In an intermediate range of the citrate concentration (about $(1-5) \times 10^{-4} \text{ M}$), the atom number is drastically decreased. Within this range, it decreases only slightly with increasing citrate concentration. The particles are well separated, although a few lumps are present; these lumps of coalesced particles may partly have been formed on the grid. The width of the size distribution, *s*, is substantially smaller than in regime 1.

(3) At high citrate concentrations ($15 \times 10^{-4} \text{ M}$ in Figure 1), a very broad size distribution is observed. At this high ionic strength, citrate already has some destabilizing effect, since many particles coalesce to form very large lumps.

At the lowest and highest citrate concentrations in Figure 1, one finds dislocations in the particles, multiple twinning, staple faults, lamella twinning, and partial dislocations; the shapes of the particles often are ellipsoidal. The particles in the intermediate citrate range are almost spherical and show little imperfections; these differences indicate different growth mechanisms in the various ranges of the citrate concentration.

The absorption spectrum of the particles formed in regime 1 contains the silver plasmon absorption band at about 385 nm and a maximum or shoulder at longer wavelengths. The latter is typical for particles that loosely stick together.⁵ At the higher citrate concentrations, the plasmon band is symmetric, which indicates that the samples do not contain many agglomerated particles, a conclusion that agrees with the electron micrograph observations.

The plasmon absorption band of the particles of regime 3 ($15 \times 10^{-4} \text{ M}$ citrate in Figure 4) is also symmetric and practically not different from the one at intermediate citrate concentration ($1.0 \times 10^{-4} \text{ M}$), although the particles at the high citrate concentration have an extraordinarily broad size distribution. This illustrates that one cannot unambiguously derive a conclusion about the quality of colloidal silver particles from the absorption spectrum alone. The reason lies in the fact that the particles in both samples studied have sizes much smaller than the wavelengths of light; Mie theory teaches that the specific absorption is independent of particle size under these conditions.⁶

High-resolution micrographs of the particles produced in the intermediate range of citrate concentration are shown in Figures 5 and 6; the insets in the upper right are the power spectra. The particles have almost no distortions. Icosahedron particles viewed along the 2-fold, 3-fold, and 5-fold symmetry axis are shown in parts a, b, and c of Figure 5, respectively. In Figure

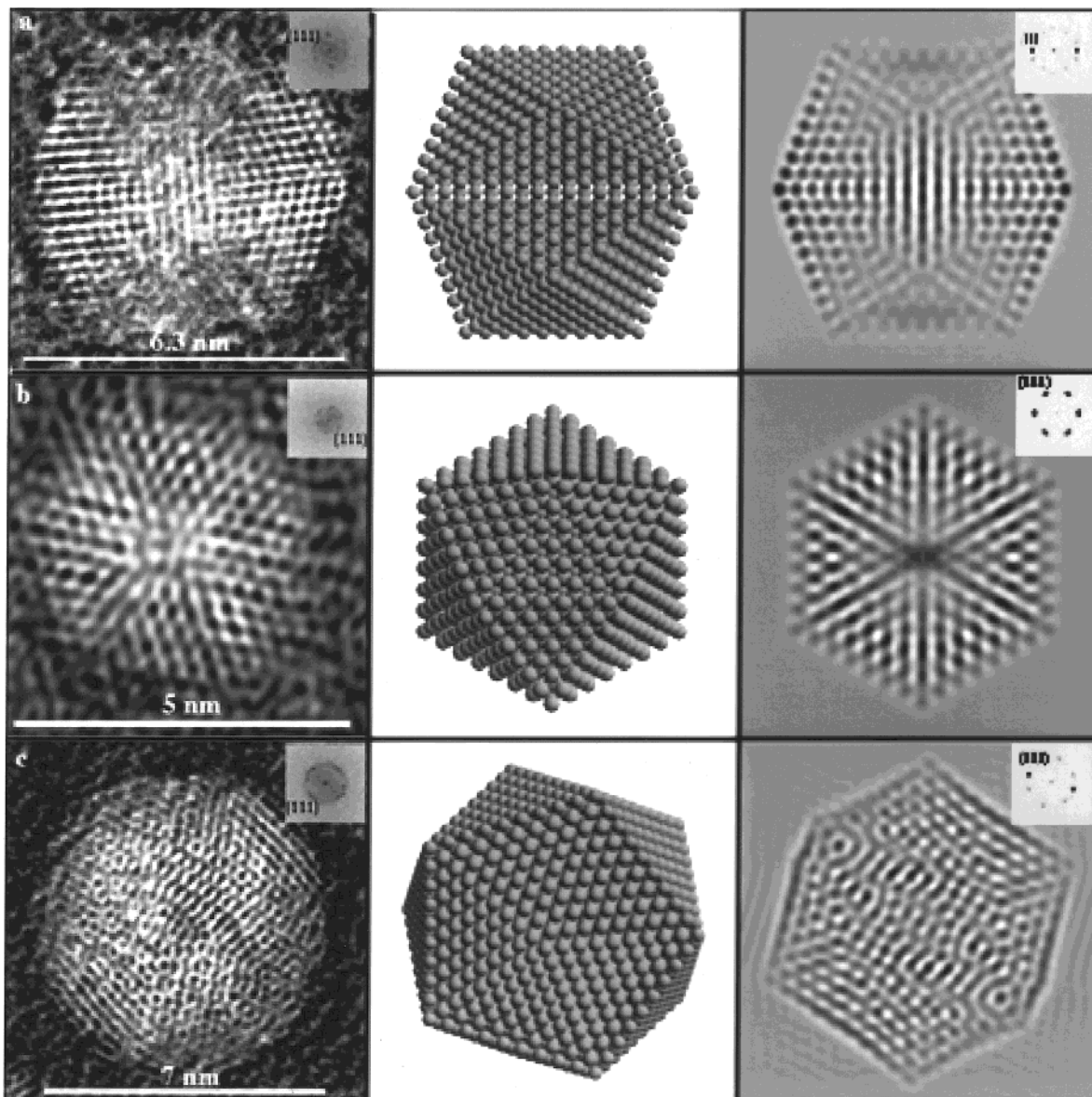


Figure 5. Left: various projections of icosahedra particles. They were produced at a citrate concentration of 1.5×10^{-4} M. The power spectra reveal (a) a strong pair of (111) reflections and two diffuse pairs of reflections, (b) three pairs of (111) reflections, (c) five pairs of the (111) family and five weaker pairs of the (200) family of reflections. Note the good agreement with the simulations consisting of ideal models calculated with molecular simulations program Cerius 3.8 (middle) and multislice calculations (right).

6, two typical views of a cuboctahedron are presented. Similar structures have been observed for silver particles produced by evaporation of silver on KCl⁷ and in computer simulations.⁸ The results of our computer simulations also are shown in Figures 5 and 6.

Figure 7 shows micrographs of the samples that were involved in a size-enlargement experiment. A 1.0×10^{-4} M silver sol was radiolytically prepared using a citrate concentration of 5.0×10^{-4} M; the particles are shown on the left side of the figure. An amount of 5 mL of this sol was now mixed with 35 mL of the original solution and irradiated until all the Ag⁺ ions were reduced; the particles, which are shown in the right side of Figure 7, are twice as large as the ones on the left side. Note that the overall silver concentration always was 1.0×10^{-4} M and that the amount of silver in the form of Ag⁺ was 7 times larger than in the form of Ag_n seeds in the second irradiation experiment. The final particles have a mass 8 times greater than the seeds, which shows that the enlargement was perfect without simultaneous formation of smaller seeds.

Discussion

Citrate exerts a drastic effect on the size and size distribution of the silver particles that are formed under otherwise constant conditions, i.e., constant Ag⁺ concentration and constant rate of reduction. Concerning the quality of the silver particles produced, there exists a rather narrow range of citrate concentration about $(1-5) \times 10^{-4}$ M, where well-separated particles with a narrow size distribution are produced. The particles formed at lower citrate concentrations have many imperfections and often consist of several crystallites. At too high a citrate concentration, large lumps often are formed because of the coalescence of destabilized particles.

The experimental observations are explained by the following mechanism, which also is schematically depicted in Figure 8. The first step of particle formation is the reduction of Ag⁺ by the 1-hydroxymethylethyl radical:



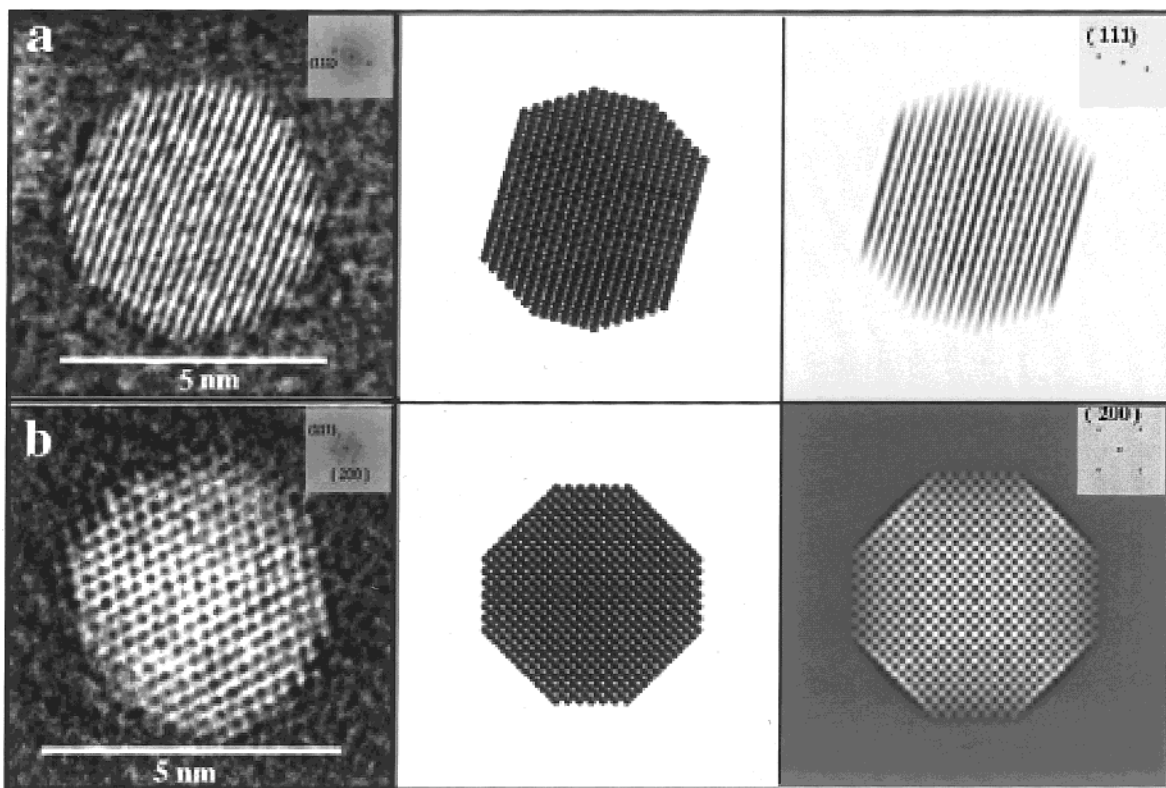


Figure 6. Left: various projections of cuboctahedra particles, with $[\text{citrate}] = 1.5 \times 10^{-4} \text{ M}$: (a) oriented along the (112) direction: (b) oriented along the (110) direction; (middle and right) computer simulations (see legend of Figure 5).

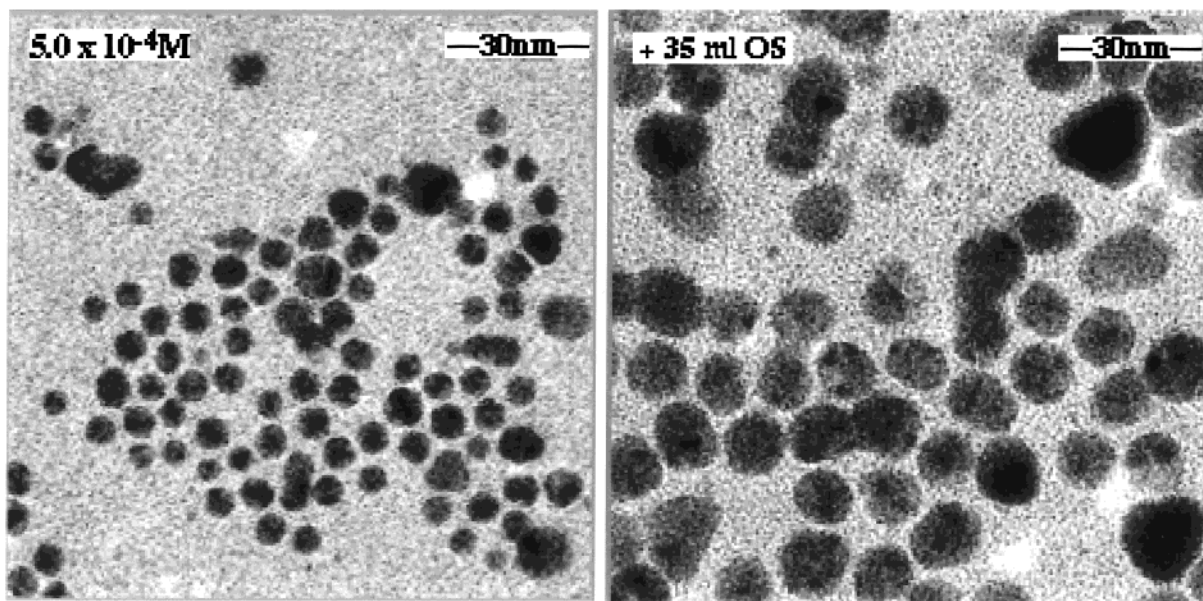


Figure 7. Particle enlargement experiment: particles before (left) and after (right) the enlargement.

The reaction is relatively slow, since the electrochemical potential of the radical is more positive than that of the Ag^+/Ag^0 system (where Ag^0 is a free silver atom in solution). This fact has previously been discussed in detail.⁹ The reaction, however, is fast enough to compete successfully with the mutual deactivation of the radicals at the dose rate used. The silver atoms form oligomeric clusters of larger and larger size via condensation reactions.¹⁰ The nature of certain intermediate clusters has been elucidated by pulse radiolysis; they generally carry a positive charge, such as Ag_2^+ , Ag_4^{2+} , Ag_9^+ , etc.¹¹ The exact structure does not matter in the present treatment; we simply designate the small clusters by Ag_x . They are complexed by citrate:



At low citrate concentrations, the positively charged clusters will more or less be neutralized, which favors their condensation to build up larger ones:



Thus, the Ag_x 's are nuclei for the formation of larger particles via condensation reactions; we designate them type-I nuclei.

At a critical size, Ag_m , the clusters almost cease to grow via this mechanism. This size is possibly reached in the range of m from 10 to 20, i.e., when the diameter is still smaller than 1

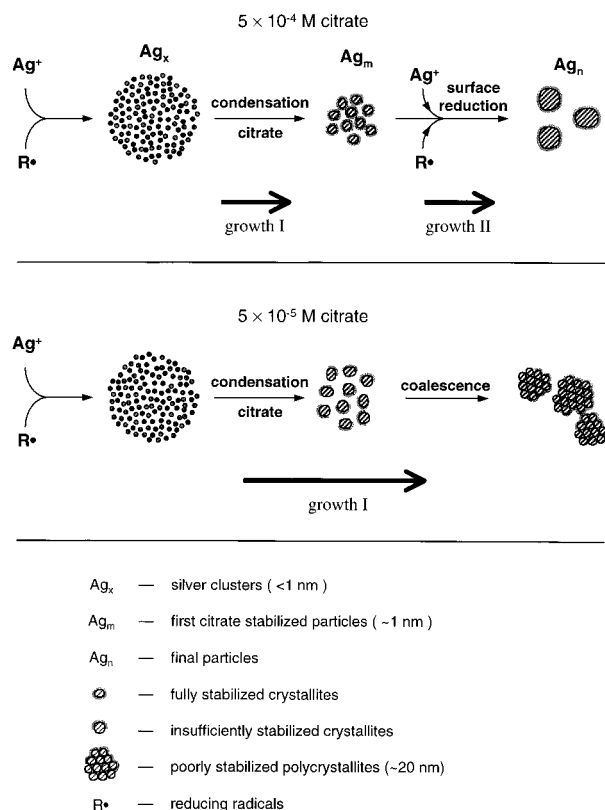
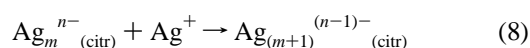
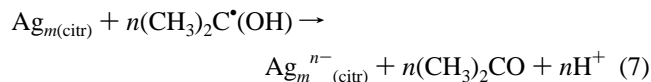


Figure 8. Illustration of important routes of particle growth at two citrate concentrations. At the higher citrate concentration, the stages of nucleation and growth are well separated. At the lower citrate concentration, coalescence reactions of growing particles contribute to particle enlargement.

nm. (In the real system, there is a distribution of x and m). At this point, the clusters behave like typical colloidal particles; i.e., they have built up a strong repelling layer of citrate, which prevents them from coming into close contact; in addition, the reactivity of the clusters to condense decreases with size, since they are under less surface pressure. The Ag_m clusters, which we designate as type-II nuclei, then grow via the reduction of silver ions on their surface. The mechanism of this reduction has been recognized already many years ago.¹² The organic radicals react via electron transfer, and Ag^+ ions are reduced by the stored electrons:



The enlargement experiment of Figure 7 demonstrates this mechanism very visibly. It is important to note that adsorbed citrate does not inhibit particle growth via this mechanism.

In the intermediate range ($(1-5) \times 10^{-4}$ M) the citrate concentration is high enough to stabilize the Ag_m clusters with respect to further growth. As the final particle size decreases slightly with increasing citrate concentration, one concludes that the atom number m in Ag_m decreases slightly; i.e., the particles are stabilized by citrate against further condensation at a smaller size. Since the specific rate of reaction 4 is rather slow, the radicals start to react according to eq 7 at an early stage of irradiation, i.e., when a sufficiently high concentration of Ag_m 's has been reached. This means that the steps of nuclei (type-II) formation and growth of the nuclei are well separated. Under

these favorable conditions, the resulting final particles are crystalline, are nicely faceted, have a narrow size distribution, and are well separated.

At too low citrate concentrations, the citrate layer is not so effectively built-up around the Ag_x clusters. Since they are not protected from further reaction with each other, when they have reached size m , they form larger and larger structures, first mainly via condensation and later via coalescence.¹⁰ Besides the growth according to eqs 7 and 8, these coalescence reactions contribute to particle enlargement to an increasing extent. Reactions 7 and 8 occur more rarely because of the very low concentration of the large structures that are formed by multiple coalescence; the radicals continue to react frequently according to eq 4, which means that new nuclei are formed during all stages of silver reduction. The steps of formation and growth of nuclei are not well separated under these conditions, and the resulting final particles are polycrystalline, have a wide size distribution, and partly stick loosely together.

Final Remarks

Few electron microscope studies have yet been made to investigate the effects of capping materials in metal ion reduction. In the present paper, rather unusual conditions exist: a low molecular weight stabilizer is used and the reduction of the metal ions occurs via free radicals that are radiolytically generated. The capping effects described here will not literally apply to other systems, especially when a polymeric stabilizer is used and the reduction occurs chemically. For example, studies of the effect of polyacrylate on the formation of platinum particles have shown that the adsorbed stabilizer strongly retards type-II growth of the particles, in contrast to the present findings.¹³

We also emphasize the preparative aspect of the present work. The radiolytic synthesis of silver particles in the intermediate range of citrate concentration yields rather perfect crystalline particles, whereas the thermal citrate reduction generally leads to colloids with a poor size distribution similar to the one in Figure 1 at 15×10^{-4} M citrate.

Acknowledgment. The authors thank Prof. Dan Meisel for valuable discussions, and Mrs. Ulli Bloeck and Mr. Marc Cozzi for technical assistance in the TEM experiments. The work described herein was supported by the Office of Basic Energy Sciences of the U.S. Department of Energy. This is Contribution No. 4142 NDRL from the Notre Dame Radiation Laboratory.

References and Notes

- (1) Enüstün, B. V.; Turkevich, J. *J. Am. Chem. Soc.* **1963**, *85*, 3317.
- (2) Turkevich, J.; Kim, G. *Science* **1970**, *169*, 873.
- (3) (a) Lee, P. C.; Meisel, D. *J. Phys. Chem.* **1982**, *86*, 3391. (b) Kamat, P. V.; Flumiani, M.; Hartland, G. V. *J. Phys. Chem.* **1998**, *102*, 3123.
- (4) Kunath, W.; Zemlin, F.; Weiss, K. *Optik* **1987**, *76*, 122.
- (5) (a) Weitz, D. A.; Lin, M. Y.; Sandroff, C. *Surf. Sci.* **1985**, *158*, 147. (b) Quinten, M.; Schönauer, D.; Kreibitz, U. *Z. Phys. D* **1989**, *12*, 521.
- (6) Kreibitz, U.; Vollmer, M. *Optical Properties of Metal Clusters*; Springer: Berlin, 1995.
- (7) Marks, L. D.; Smith, D. J. *J. Cryst. Growth* **1981**, *54*, 425.
- (8) (a) Kirkland, A. I.; Jefferson, D. A.; Tang, D.; Edwards, P. P. *Proc. R. Soc. London, Ser. A* **1991**, *434*, 279. (b) Urban, J.; Sack-Kongehl, H.; Weiss, K. *Z. Phys. D* **1993**, *28*, 247. (c) Urban, J.; Sack-Kongehl, H.; Weiss, K. *High Temp. Mater. Sci.* **1996**, *36*, 155.
- (9) Henglein, A. *Chem. Mater.* **1998**, *10*, 444.
- (10) The notion "condensation" is used here for particles that combine to form tiny crystallites; the notion "coalescence" is used for combining particles to form larger structures in which the particles more or less preserve

their individual crystallinity. The notion "cluster" is used for small oligomeric silver species, which behave like molecules, whereas the notion "particle" is used when it behaves like a colloid, i.e., possesses a repelling layer of adsorbed citrate.

(11) Ershov, B. G.; Janata, E.; Henglein, A. *J. Phys. Chem.* **1993**, *97*, 339.

(12) (a) Henglein, A. *J. Phys. Chem.* **1979**, *83*, 2209. (b) Meisel, D. *J. Am. Chem. Soc.* **1979**, *101*, 6133. (c) Henglein, A. *J. Phys. Chem.* **1980**, *84*, 3461. (d) Henglein, A.; Lilie, J. *J. Am. Chem. Soc.* **1981**, *103*, 1059.

(13) (a) Ahmadi, T. S.; Wang, Z. L.; Green, T. C.; Henglein, A.; El-Sayed, M. A. *Science* **1996**, *272*, 1924. (b) Petroski, J. M.; Wang, Z. L.; Green, T. C.; El-Sayed, M. A. *J. Phys. Chem. B* **1998**, *102*, 3316.